TWO DIMENSION DIGITAL BEAMFORMING PREPROCESSING IN MULTIBEAM SCANSAR

Pingping Huang[1, *], Wei Xu[2], and Weikong Qi[3]

[1]College of Information Engineering, Inner Mongolia University of Technology, Hohhot 010051, China

[2]Department of Spaceborne Microwave Remote Sensing, Institute of Electronics, Chinese Academy of Sciences (IECAS), Beijing 100190, China

[3]China Academy of Space Technology, Beijing, China

Abstract—The novel multibeam ScanSAR takes advantage of the displaced phase center multiple azimuth beam (DPCMAB) imaging scheme and intra-pulse beam steering in elevation in ScanSAR to achieve the high-resolution ultra-wide-swath imaging capacity. This letter proposes an innovative two-dimensional (2D) digital beamforming (DBF) space-time preprocessing approach for multibeam ScanSAR. According to echo proprieties of such imaging scheme, both azimuth ambiguity and range ambiguity problems should be resolve before a conventional ScanSAR imaging processor. After range compressing in each receive channel, a 2D DBF processor is carried out in the range-Doppler domain. The azimuth DBF operation is adopted to resolve the azimuth nonuniform sampling problem in multichannel SAR systems, while the DBF preprocessing in elevation is carried out to separate echoes from different subswaths corresponding to different sub-pulses. Imaging results on simulated distributed targets validate the proposed 2D DBF preprocessing approach.

1. INTRODUCTION

Spaceborne synthetic aperture radar (SAR), as a high resolution microwave remote sense system, is experiencing a golden age and proved to be an extremely useful surveillance tool for military applications, terrain measurement, ocean application, agricultural

* Corresponding author: Pingping Huang (dzspph@gmail.com).

surveillance and other useful applications [1, 2]. However, the modern generation of spaceborne SAR systems suffers a basic constraint between high azimuth resolution and wide swath coverage. For example, the sliding spotlight and spotlight modes are operated for a high geometric resolution at cost of the reduced swath width [2–5], while ScanSAR [6, 7] and Terrain Observation by Progressive Scans (TOPS) [8–10] are adopted for the wide swath coverage but with an impaired azimuth resolution.

However, future spaceborne microwave remote sensing missions will require a complete and frequent coverage of the Earth with a reasonably high geometric resolution [11], e.g., a swath width of more than 400 km with an azimuth resolution of well 10 m [12–14]. To implement such advanced imaging capacity, ScanSAR or TOPS with the displace phase center multiple azimuth beam (DPCMAB) technique is proposed [12–18]. In this mode, an high-resolution ultra-wide-swath imaging capacity of a swath coverage of 400 km simultaneously with an azimuth geometric resolution of 5 m, while the height of the orbit is 630 km [14]. In order to further improve the high-resolution width-swath (HRWS) imaging capacity, multichannel ScanSAR with intra-pulse beam steering on transmit in elevation is proposed [19, 20]. Compared with conventional multichannel ScanSAR, this novel imaging scheme named as multibeam ScanSAR obtains a better azimuth resolution with the same swath width, since multiple subswaths are illuminated by several sub-pulses in sequence in a single pulse repetition interval (PRI) via intra-pulse beam steering on transmit in elevation.

In multichannel SAR systems with multiple azimuth sub-apertures, to generate the uniform sampling of the whole azimuth received signals, the optimum PRF should be chosen and given as follows [21–23]:

$$\text{PRF}_{opt} = \frac{2v_s}{N \cdot \Delta x} \tag{1}$$

where v_s is the sensor velocity, Δx the along-track offset, and N the number of sub-apertures in azimuth. Such a rigid selection of the PRF value will be in conflict with the timing diagram selection and increasing PRF of improved azimuth ambiguity energy suppression, especially in the burst mode. An azimuth DBF processor with null-steering could be adopted to reconstruct azimuth multichannel raw data in the case of azimuth nonuniform sampling [22–24]. Moreover, echoes from different subswaths corresponding to different transmitted sub-pulses are temporally superimposed at radar receivers. Fortunately, the temporal overlap of echoes can be resolved in the spatial domain by DBF on receive, where we exploit the relation

between the time delay and the elevation angle in the sidelooking radar imaging geometry [19].

According to echo properties of multibeam ScanSAR, this letter proposes an innovative 2D DBF processor for multibeam ScanSAR data preprocessing before a monstatic SAR focusing processor. To well separate echoes from different subswaths, raw data of each receive channel should be compressed in the range direction at first. Afterward, a 2D DBF processor is carried out in the range-Doppler domain to reconstruct the nonuniform sampling azimuth data and separate echoes from different subswaths.

This paper is organized as follows. Section 2 reviews the imaging scheme of the novel multibeam ScanSAR mode. Section 3 focuses on presenting the proposed 2D DBF processing approach. A simulation experiment on distributed targets is carried out to validate the proposed approach in Section 4. Finally, this letter is concluded in Section 5.

2. MULTIBEAM SCANSAR

Future spaceborne SAR missions require an ultra wide swath unambiguous coverage of the Earth with a high geometric resolution, for example imaging a swath 400 km with a resolution below 5 m. Besides taking advantage of the DPCMAB technique in ScanSAR, the mapping of such swath width with a short antenna still requires a large number of bursts. The increased number of bursts will impair the system performances and leads to conflict with regard of the achievable azimuth resolution. Such problems could be resolved by a simultaneous mapping of multiple subswaths during each burst as shown in Fig. 1.
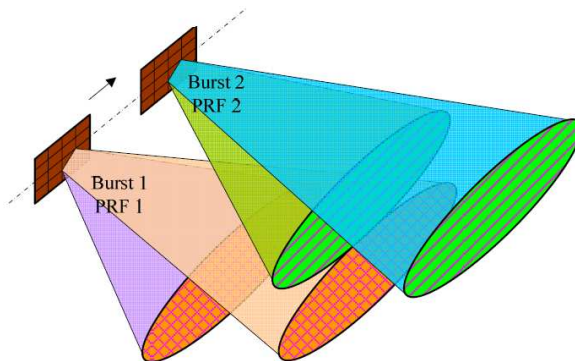

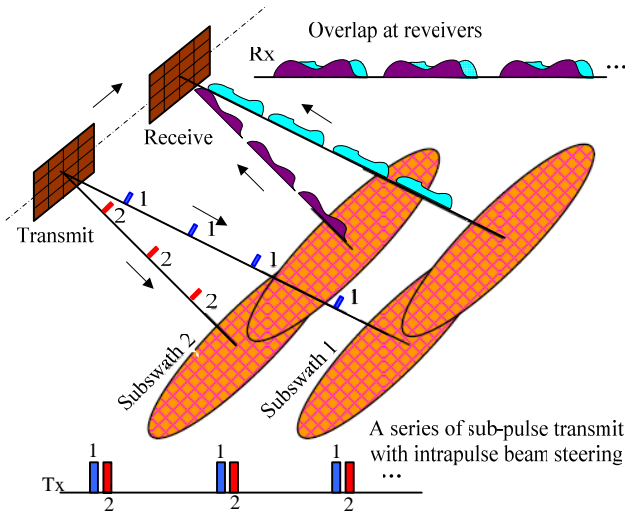**Figure 1.** ScanSAR imaging with multiple beams in elevation.

Figure 2. A series of sub-pulses are transmitted with intrapulse beam steering, while echoes form different subswaths are overlap at receivers.

To obtain a simultaneous mapping of multiple subswaths during each burst, multiple subswaths are illuminated by a series of sub-pulses with a sequence of narrow and high-gain transmit antenna beams. This operated technique is named as intrapulse beam steering in elevation, and also called as multidimensional waveform encoding in elevation. Usually, we start from a far range illumination and subsequently proceed the near range to shorten the receiving window length. However, in multibeam ScanSAR, we may start from a near range illumination and subsequently proceed the far range, since different subswaths usually corresponds to different sub-pulses in different pulse repetition intervals (PRIs) in multibeam ScanSAR as shown in Fig. 2. In Fig. 2, the sub-pulse 1 is transmitted to the far range subswath 1, while the sub-pulse 2 is transmitted to the near range subswath 2. The number of emitted pulses between radar and the imaged scene is 4 in subswath 1 and is 3 in subswath 2. To obtain the almost same system performances in different subswaths, sub-pulses transmitted in a single PRI could be transmitted with different pulse duration, bandwidths and peak power. As a result, this elevation illumination strategy may reduce the overall power requirements for a given signal to noise ratio (SNR).

However, echoes from all subswaths will be received by each elevation sub-aperture, and echoes from different subswaths are superimposed at each receiver as shown in Fig. 2. The temporal overlap

problem of echoes from different subswaths could be resolved in the spatial domain by DBF with mull steering in elevation based on the relation between the time delay and the elevation angle in the side looking SAR imaging geometry.

Besides separating echoes from different subswaths, the nonuniform azimuth sampling in the DPCMAB SAR systems should be overcome. This ambiguity problem could also be resolved by a DBF processor with null steering. Therefore, we propose a 2D DBF processor to resolve both range and azimuth ambiguity problems.

3. AZIMUTH DATA PROCESSING APPROACH

This section is focused on presenting the proposed 2D DBF processor to deal with multibeam ScanSAR raw data. A simple example of the total receive antenna with multiple sub-apertures is shown in Fig. 3. The sub-aperture Tx is used to transmit radar pulses, while Rx_{mn} is the receive sub-aperture. The subscript m indicates the sequence number of the row, while the subscript n denotes the sequence number of the column.

To separate received echoes from different subswaths and reconstruct azimuth multichannel nonuniform sampling signal, the proposed 2D processor should be operated in the range Doppler domain. Moreover, the power of the revived echoes of each point target is distributed in the whole pulse duration, which leads to that it is hard to separate two signals in the spatial domain via a DBF processor, since
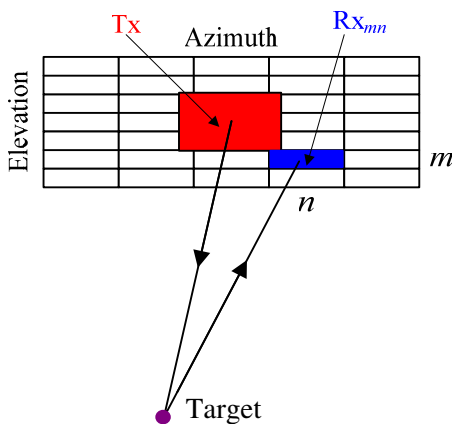

Figure 3. The whole antenna with multiple sub-apertures in both azimuth and elevation.
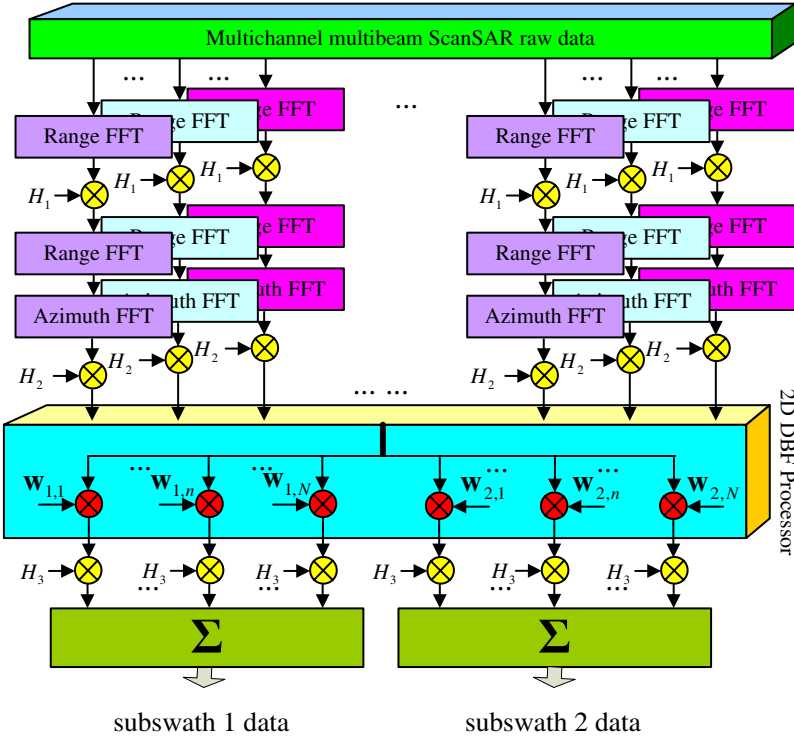
Figure 4. The block diagram of the proposed 2D preprocessing processor.

the large signal duration corresponds to the large elevation angular interval. As a result, the range compression should be first taken in each receive channel before DBF processing in the range Doppler domain. The block diagram of the proposed preprocessing approach via a 2D DBF processor is shown in Fig. 4.

Assumed the transmitted waveform is the linear frequency modulation (LFM) signal, baseband echoes received by the sub-aperture Rx_{mn} is:

$$ss_{mn}(t, \tau) = \sum_{k=1}^{2} G(\theta, \varphi_k) \cdot \exp\left[j\pi K_r \left(\tau - \tau_k - \frac{R_k + R_{mn,k}}{c}\right)^2\right]$$

$$\cdot \exp\left(-j2\pi \frac{R_k + R_{mn,k}}{\lambda} - j2\pi f_c \tau_k\right) \tag{2}$$

with

$$R_k(t) = \sqrt{v^2 t^2 + R_0^2} \tag{3}$$

$$R_{mn,k}(t) \approx \sqrt{(vt - \Delta x_n)^2 + R_0^2} \tag{4}$$

where $G(\theta, \varphi_k)$ indicates the 2D antenna pattern, θ is the squinted angle in azimuth, φ_k is the antenna arriving angle in elevation, f_c is the carrier frequency, c is the light speed, the subscript k $(k = 1, 2)$ is used to distinguish different transmitted sub-pulses, K_r is the transmitted pulse chirp rate, τ is the range time, τ_k is the delay between two transmitted sub-pulses, R_k and $R_{mn,k}$ are the range from target to the transmit sub-aperture Tx and receive Rx$_{mn}$, respectively, R_0 is the slant range, Δx_n is the physical along-track distance between the transmit sub-aperture Tx and the receive sub-aperture Rx$_{mn}$. After range Fast Fourier Transform (FFT) of received baseband echoes in each channel, the form of (4) in the range frequency domain can be expressed as follows.

$$sS_{mn}(t, f_r) = \sum_{k=1}^{2} G(\theta, \varphi_k) \cdot \exp\left[-j2\pi f_r \left(\tau_k + \frac{R_k + R_{mn,k}}{c}\right)\right]$$
$$\cdot \operatorname{rect}\left[\frac{f_r}{B_{r,k}}\right] \cdot \exp\left(-j\pi \frac{f_r^2}{K_r}\right) \cdot \exp\left(-j2\pi \frac{R_k + R_{mn,k}}{\lambda}\right) \tag{5}$$

The matched filter $H_1(f)$ for range compression as shown in Fig. 3 is as follows:

$$H_1(f) = \exp\left(j\pi f_r^2 / K_r\right) \cdot \operatorname{rect}\left[\frac{f_r}{B_r}\right] \tag{6}$$

where f_r is the range frequency and B_r the transmitted pulse bandwidth. After the range inverse FFT (IFFT), the received signal can be rewritten as:

$$ss(t, \tau) = \sum_{k=1}^{2} G(\theta, \varphi_k) \cdot \operatorname{sinc}\left(\tau - \tau_k - \frac{R_k + R_{mn,k}}{c}\right) \cdot \exp\left(-j2\pi \frac{R_k + R_{mn,k}}{\lambda}\right)$$
$$\approx \sum_{k=1}^{2} G(\theta_a, \varphi_k) \cdot \operatorname{sinc}\left(\tau - \tau_k - \frac{R_k + R_{1n,k}}{\lambda}\right) \cdot \exp\left(-j2\pi \frac{R_k + R_{1n,k}}{\lambda}\right)$$
$$\cdot \exp\left[-j2\pi \frac{(m-1)d_r \sin \varphi_k}{\lambda}\right]$$
$$\approx \sum_{k=1}^{2} G(\theta_a, \varphi_k) \cdot \operatorname{sinc}\left(\tau - \tau_k - \frac{R_k + R_{1n,k}}{\lambda}\right) \cdot \exp\left[-j\frac{4\pi}{\lambda} R_0\right]$$

$$\cdot \exp\left[-j\frac{\pi \cdot \Delta x_n^2}{2\lambda R_0}\right] \cdot \exp\left[-j\frac{2\pi v^2}{\lambda R_0}\left(t-\frac{\Delta x_n}{2v}\right)^2\right] \cdot \exp\left[-j2\pi\frac{(m-1)d_r\sin\varphi_k}{\lambda}\right] \quad (7)$$

After taking the azimuth FFT, the signal in the range-Doppler domain can be computed as follows:

$$Ss(f_a, \tau) = \sum_{k=1}^{2} G(\theta, \varphi_k) \cdot \text{sinc}\left(\tau - \tau_k - \frac{R_k + R_{1n,k}}{c}\right) \cdot \exp\left[-j\frac{4\pi}{\lambda}R_0\right]$$

$$\cdot \exp\left[-j\frac{\pi \cdot \Delta x_n^2}{2\lambda R_0}\right] \cdot \exp\left[-j\pi\frac{\lambda R_0}{2v^2}f_a^2\right] \cdot \exp\left[-j2\pi f_a\frac{\Delta x_n}{2v}\right]$$

$$\cdot \exp\left[-j2\pi\frac{(m-1)d_r\sin\varphi_k}{\lambda}\right] \quad (8)$$

The following transfer function is multiplied to remove the constant phase shift caused by the DPCMAB SAR imaging scheme and the constant azimuth linear frequency modulation for the whole received signal.

$$H_{2,n}(f_a) = \exp\left[j\frac{\pi \cdot \Delta x_n^2}{2\lambda R_0}\right] \cdot \exp\left[j\pi\frac{\lambda R_0}{2v^2}f_a^2\right] \quad (9)$$

Afterwards, the received signal is rewritten as follows:

$$Ss(f_a, \tau) = \sum_{k=1}^{2} G(\theta, \varphi_k) \cdot \text{sinc}(\tau - \tau_k - \tau_d) \cdot \exp\left[-j\frac{4\pi}{\lambda}R_0\right]$$

$$\cdot \exp\left[-j2\pi f_a\frac{\Delta x_n}{2v}\right] \cdot \exp\left[-j2\pi\frac{(m-1)d_r\sin\varphi_k}{\lambda}\right] \quad (10)$$

Therefore, the compact characterization of the multibeam ScanSAR system can be described by the two-dimensional steering vector as follows:

$$\mathbf{u} = \exp\left[-j2\pi\frac{\Delta\mathbf{x}}{\lambda}\sin(\theta) - j2\pi\frac{\mathbf{d_{r,m}}}{\lambda}\sin\varphi_k\right]^T \quad (11)$$

with

$$\Delta\mathbf{x} = [\Delta x_1, \Delta x_2, \ldots, \Delta x_N]^T \quad (12)$$

$$\mathbf{d_{r,m}} = d_r \cdot [0, 1, 2, \ldots, M-1]^T \quad (13)$$

where $(\cdot)^T$ denotes the matrix transpose operator, N the number of sub-apertures in azimuth, and M the number of sub-apertures in elevation. Thus, the two-dimensional steering vector could be

expressed as the Kronecker product of azimuth and range steering vectors as follows:

$$\mathbf{u}_k(\varphi_k) = \exp\left[-j2\pi\frac{\boldsymbol{\Delta}\mathbf{x}}{\lambda}\sin(\theta)\right] \otimes \exp\left[-j2\pi\frac{\mathbf{d}_{\mathbf{r,m}}}{\lambda}\sin\varphi_k\right] \quad (14)$$

where $\otimes$ is the Kronecker product operator, and $\mathbf{u}_k(\varphi_k)$ is a $MN \times 1$ vector. Define a matrix $\mathbf{U}$ as follows

$$\mathbf{V} = [\mathbf{v}_1(\varphi_1), \mathbf{v}_2(\varphi_2)]_{MN \times 2N} \quad (15)$$

with

$$\mathbf{v}_k(\varphi_k) = [\mathbf{u}_k(f_a), \mathbf{u}_k(f_a + \mathrm{PRF}), \ldots, \mathbf{u}_k(f_a + (N-1) \cdot \mathrm{PRF})]_{MN \times N}$$
$$f_a \in \left[-\frac{N-1}{2} \cdot \mathrm{PRF}, -\frac{N-3}{2} \cdot \mathrm{PRF}\right] \quad (16)$$

It is assumed that the multiplied weighting matrix is $\mathbf{W}_{MN \times 2N}$. The k-th column steering vector of $\mathbf{W}_{MN \times 2N}$ is defined as $\mathbf{w}_k$ which makes that the position of the corresponding the azimuth angle and the elevation look angle equals to one, while positions of other ambiguities including Doppler ambiguity and range ambiguity equal to zeros. Thereby, the desired signal can be extracted through the following formulation:

$$\mathbf{w}_k^H \mathbf{V} = \mathbf{H}_k \quad (17)$$

where $(\cdot)^H$ denotes the matrix conjugate transpose operator, and $\mathbf{H}_k$ is the vector $[h_1, h_2, \ldots, h_{2N}]^T$ with $h_k = 1$ and other elements are zero. According to (17), the multiplied weighting vector $\mathbf{w}_k$ could be expressed as follows:

$$\mathbf{w}_k = (\mathbf{H}_k \mathbf{V}^+)^H \quad (18)$$

where $(\cdot)^+$ denotes the pseudo-inverse operation. The weighting vector $\mathbf{w}_k$ and the signal vector $\mathbf{u}_k(\varphi_k)$ are multiplied to achieve de-blurred signal vector $\mathbf{Y}$ as follows:

$$\mathbf{Y} = \mathbf{W}^H \mathbf{u}_k(\varphi_k) = \mathbf{H}(\varphi_k) \quad (19)$$

Before the subsequent coherent combination of multiple Doppler spectrums on different sub-bands with a width of PRF, a linear Doppler frequency modulation is introduced via the following transfer function:

$$H_3(f_a) = \exp\left[-j\pi\frac{\lambda R_0}{2v^2}f_a^2\right] \quad (20)$$

Afterward, N signals with the same elevation view angle are obtained from 2 by N de-blurred matrix $\mathbf{Y}$, and then they are arranged in the Doppler domain and combined coherently to achieve the whole Doppler spectrum which is the desired unambiguous signal from each subswath.
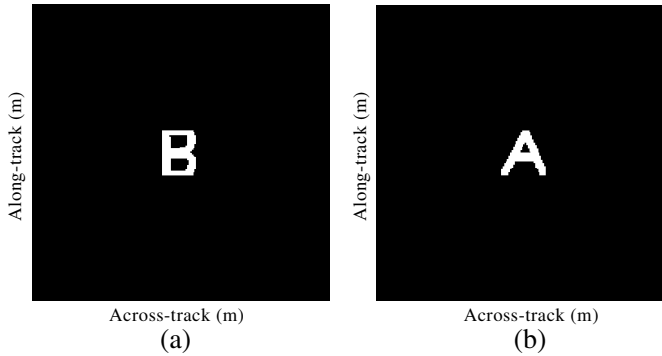
Figure 5. Two dstributed imaged targets in different subswaths. (a) Target 1 in the center of subswath 1. (b) Target 2 in the center of subswath 2.

Table 1. Simulation parameters.

PARAMETERS	Value
Carrier frequency	9.65 GHz
Orbit height	514.8 km
Satellite velocity	7608 m/s
Pulse duration	20 μs
The transmit time delay	30 μs
Signal bandwidth	30 MHz
Sampling frequency	50 MHz
Transmit antenna length	2.8 m
Receive antenna length	2.4 m*3
Transmit antenna height	0.176 m
Receive antenna height	0.44 m*4
Look angle (subswath 1)	$34.5° \sim 41.5°$
Look angle (subswath 2)	$20.0° \sim 31.3°$
Slant range (subswath 1)	637.06 km $\sim$ 710.60 km
Slant range (subswath 2)	550.80 km $\sim$ 611.76 km

4. SIMULATION EXPERIMENT

To validate the proposed 2D DBF preprocessing approach for multibeam ScanSAR, a simulation experiment on distributed targets is carried out in this section. All system parameters are listed in Table 1.
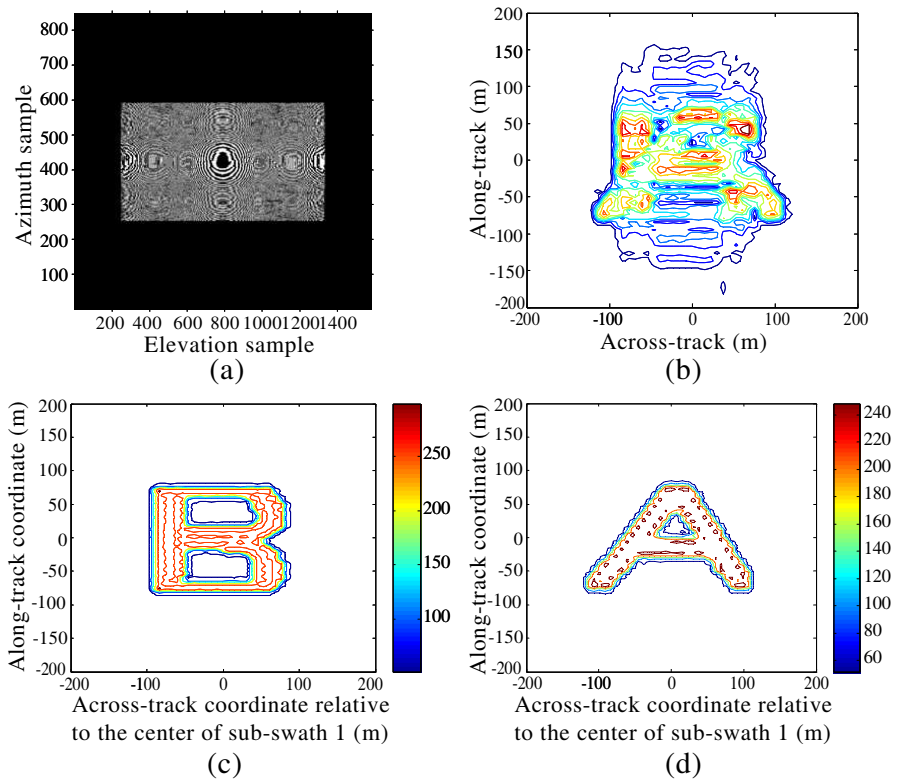
Figure 6. Simulation results on distributed targets. (a) Received echoes in a sub-aperture. (b) Simulation result in a sub-aperture without any preprocessing. (c) Imaging result of target 1 via the proposed approach. (d) Imaging result of target 2 via the proposed approach.

There are two distributed targets in different subswaths as shown in Fig. 5. Echoes of two distributed targets are completely overlapped at each receiver as shown in Fig. 6(a). Fig. 6 shows imaging results without any preprocessing and with the proposed approach. It can be clearly seen that both targets are well focused via the proposed 2D DBF approach, and simulation results validate the processing approach.

5. CONCLUSION

The multibeam ScanSAR may be adopted for future spaceborne high resolution ultra wide swath imaging, since it achieves the

HRWS imaging capacity better than conventional multichannel ScanSAR under the same condition. However, both the temporal overlap of echoes from different subswaths corresponding to different sub-pulses at receivers and the nonumiform azimuth sampling in conventional multichannel SAR systems arise the difficulty of signal processing for multibeam ScanSAR. According to echo properties in multibeam ScanSAR, this letter proposes an innovative 2D DBF preprocessing approach before the monostatic SAR imaging processors. Imaging results on simulated distributed targets validate the proposed approach.

ACKNOWLEDGMENT

REFERENCES

1. Curlander, J. C. and R. N. McDonough, *Synthetic Aperture Radar: Systems and Signal Processing*, John Wiley & Sons, New York, 1991.

2. Franceschetti, G. and R. Lanari, *Synthetic Aperture Radar Processing*, CRC Press, New York, 1999.

3. Guo, D., H. Xu, and J. Li, "Extended wavenumber domain algorithm for highly squinted sliding spotlight SAR data processing," *Progress In Electromagnetics Research*, Vol. 114, 17–32, 2011.

4. An, D. X., Z.-M. Zhou, X.-T. Huang, and T. Jin, "A novel imaging approach for high resolution squinted spotlight SAR based on the deramping-based technique and azimuth NLCS principle," *Progress In Electromagnetics Research*, Vol. 123, 485–508, 2012.

5. Park, S.-H., J.-I. Park, and K.-T. Kim, "Motion compensation for squint mode spotlight SAR imaging using efficient 2D interpolation," *Progress In Electromagnetics Research*, Vol. 128, 503–518, 2012.

6. Moore, R. K., J. P. Claassen, and Y. H. Lin, "Scanning spaceborne synthetic aperture radar with integrated radiometer," *IEEE Trans. Aerosp. Electron. Syst.*, Vol. 17, No. 3, 410–420, May 1981.

7. Monti Guarnieri, A. and C. Prati, "ScanSAR focussing and interferometry," *IEEE Trans. Geosci. Remote Sens.*, Vol. 34, No. 4, 1029–1038, Jul. 1996.

8. De Zan, F. and A. Monti Guarnieri, "TOPSAR: Terrain observation by progressive scans," *IEEE Trans. Geosci. Remote Sens.*, Vol. 44, No. 9, 2352–2360, Sep. 2006.

9. Meta, A., J. Mittermayer, P. Prats, R. Scheiber, and U. Steinbrecher, "TOPS imaging with TerraSAR-X: Mode design and performance analysis," *IEEE Trans. Geosci. Remote Sens.*, Vol. 48, No. 2, 759–769, Feb. 2010.

10. Xu, W., P. Huang, Y. Deng, J. Sun, and X. Shang, "An efficient approach with scaling factors for TOPS mode SAR data focusing," *IEEE Geosci. Remote. Sens. Lett.*, Vol. 8, No. 5, 929–933, Sep. 2011.

11. Currie, A. and M. A. Brown, "Wide-swath SAR," *Proc. Inst. Electr. Eng. F — Radar Signal Process.*, Vol. 139, No. 2, 122–135, Apr. 1992.

12. Gebert, N., G. Krieger, and A. Moreira, "Multi-channel ScanSAR for high-resolution ultra-wide-swath imaging," *Proc. EUSAR*, Friedrichshafen, Germany, 2008.

13. Gebert, N., G. Krieger, M. Younis, F. Bordoni, and A. Moreira, "Ultra wide swath imaging with multi-channel ScanSAR," *Proc. IEEE IGARSS*, 21–24, Boston, MA, Jul. 2008.

14. Gebert, N., G. Krieger, and A. Moreira, "Multichannel azimuth processing in ScanSAR and TOPS mode operation," *IEEE Trans. Geosci. Remote Sens.*, Vol. 48, No. 7, 564–592, Jul. 2010.

15. Chen, J., J. Gao, Y. Zhu, W. Yang, and P. Wang, "A novel image formation algorithm for high-resolution wide-swath spaceborne SAR using compressed sensing on azimuth displacement phase center antenna," *Progress In Electromagnetics Research*, Vol. 125, 527–543, 2012.

16. Li, J., S. Zhang, and J. Chang, "Applications of compressed sensing for multiple transmitters multiple azimuth beams SAR imaging," *Progress In Electromagnetics Research*, Vol. 127, 259–275, 2012.

17. Xu, W., P. P. Huang, and Y.-K. Deng, "MIMO-tops mode for high-resolution ultra-wide-swath full polarimetric imaging," *Progress In Electromagnetics Research*, Vol. 121, 19–37, 2011.

18. Xu, W., P. Huang, and Y.-K. Deng, "Multi-channel SPCMB-tops SAR for high-resolution wide-swath imaging," *Progress In Electromagnetics Research*, Vol. 116, 533–551, 2011.

19. Krieger, G., N. Gebert, and A. Moreira, "Multidimensional waveform encoding: A new digital beamforming technique for synthetic aperture radar remote sensing," *IEEE Trans. Geosci.*

Remote Sens., Vol. 46, No. 1, 31–46, Jan. 2008.

20. Krieger, G., N. Gebert, M. Younis, F. Bordoni, A. Patyuchenko, and A. Moreira, "Advanced concepts for ultra-wide-swath SAR imaging with high azimuth resolution," *Proc. EUSAR*, Friedrichshafen, Germany, 2008.

21. Krieger, G., N. Gebert, and A. Moreira, "Unambiguous SAR signal reconstruction from nonuniform displaced phase center sampling," *IEEE Geosci. Remote Sens. Lett.,* Vol. 1, No. 4, 260–264, Oct. 2004.

22. Gebert, N., G. Krieger, and A. Moreira, "High resolution wide swath SAR imaging with digital beamforming — Performance analysis, optimization and system design," *Proc. EUSAR*, Dresden, Germany, 2006.

23. Gebert, N., G. Krieger, and A. Moreira, "Digital beamforming on receive: Techniques and optimization strategies for high-resolution wideswath SAR imaging," *IEEE Trans. Aerosp. Electron. Syst.*, Vol. 54, No. 2, 564–592, Apr. 2009.

24. Li, Z., H. Wang, T. Su, and Z. Bao, "Generation of wide-swath and high-resolution SAR images from multichannel small spaceborne SAR systems," *IEEE Geosci. Remote. Sens. Lett.*, Vol. 2, No. 1, 82–86, Jan. 2005.